



HAL
open science

A new climatic chamber adapted to the mini-centrifuge for simulating soil drying

Pm Castiblanco, Catalina Lozada, Bernardo Caicedo, Luc Thorel

► **To cite this version:**

Pm Castiblanco, Catalina Lozada, Bernardo Caicedo, Luc Thorel. A new climatic chamber adapted to the mini-centrifuge for simulating soil drying. EUROFUGE 2016, 3rd European conference on Physical Modelling in Geotechnics, Jun 2016, NANTES, France. pp.111-115. hal-01358216

HAL Id: hal-01358216

<https://hal.science/hal-01358216v1>

Submitted on 31 Aug 2016

HAL is a multi-disciplinary open access archive for the deposit and dissemination of scientific research documents, whether they are published or not. The documents may come from teaching and research institutions in France or abroad, or from public or private research centers.

L'archive ouverte pluridisciplinaire **HAL**, est destinée au dépôt et à la diffusion de documents scientifiques de niveau recherche, publiés ou non, émanant des établissements d'enseignement et de recherche français ou étrangers, des laboratoires publics ou privés.

A new Climatic Chamber adapted to the mini-centrifuge for simulating Soil Drying

P.M. Castiblanco, C. Lozada & B. Caicedo
Universidad de Los Andes, Bogotá, Colombia

L. Thorel
IFSTTAR, Point 87, Route de, Bouaye BP4129, 44341 Bouguenais cedex, France

ABSTRACT: Drought is one of the extreme events that is expected to occur with greater frequency in the world affecting soil and foundation structures. This phenomenon depends on the water content in the soil and variables such as temperature, wind velocity, and sun radiation. To simulate the effect of these variables on soil, climatic chambers have been created; however, there are no studies that include all the environmental variables that generate desiccation in soil layers. In this work, a new climatic chamber adapted to the mini-centrifuge has been designed. This chamber consists of two connected containers. The first one is designed to contain water with salt in order to control the relative humidity; the second one is designed to contain the soil and to receive the airflow. In addition, air and soil are heated with three infrared lamps simulating sun radiation. This paper describes the design of the chamber, operation ranges, facilities and preliminary results.

1 INTRODUCTION

Soil desiccation is caused by the change of environmental variables that lead to drought. This phenomenon depends on changes in the regime of subsoil water and the soil moisture, and factors such as temperature, wind velocity, and sun radiation (IPCC, 2014). The water flow within the soil is affected in great measure by these variables and therefore generate variations in stability and charge capacity. In clayey soils specially, the loss of moisture causes a raise in the stress forces giving place to cracks (Nahlawi & Kodikara 2006, Thusyanthan et al. 2007, Abu-Hejleh & Znidarčić 1995).

Crack formation has been studied by several authors using laboratory experiments where environmental factors such as temperature, relative humidity, sun radiation, and wind velocity are involved (Trabelsi et al. 2012, Corte & Higashi 1960, Nahlawi & Kodikara 2006, Miller et al. 1998, Vesga, et al, 2003, Song et al. 2013). However, most of these studies do not couple the effect of all the variables simultaneously.

In order to study the effect of environmental variables, climatic chambers have been adapted to the geotechnical centrifuge in order to scale the soil properties and variables to real conditions (Take & Bolton 2002, Caicedo et al. 2010); nevertheless, the focus of these research does not include desiccation process or crack formation.

The aim of this work is to study the crack formation and the desiccation phenomenon of clays due

to changes in sun radiation, relative humidity and wind velocity. Unlike previous works, all the variables are coupled thanks to the construction of a climatic chamber. Also, with the usage of the centrifuge the soil samples can be under accelerations up to 200×G allowing to have results closer to the ones under real stress conditions.

2 THE CLIMATIC CHAMBER FOR MODELLING SOIL DESICCATION

2.1 *Experimental setup*

The centrifuge used in this research is located in the Geotechnical models laboratory of the Universidad de los Andes in Bogota, Colombia. It allows the study of the behavior of geotechnical structures at a reduced scale (see Figure 1).

The effective radius of the mini-centrifuge is 565 mm and it can accelerate a 4 kg model up to 200×G. The strong boxes located in the arm of the centrifuge are 70 mm wide, 140 mm long, and 120 mm high.

Table 1. Properties of Speswhite kaolin clay (Lozada et al. 2015)

	Value
Liquidity limit	55 %
Plasticity limit	30 %
Specific gravity	2.6

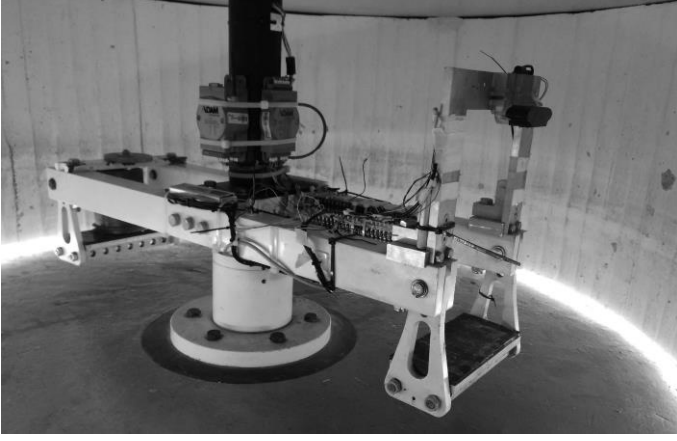


Figure 1. Mini-centrifuge. Geotechnical models laboratory, Los Andes University.

The soil used in this work is Speswhite kaolin clay prepared from a slurry state with a water content of 1.5 liquidity limit. The properties of the soil are shown in Table 1.

2.2 Climatic chamber design and acquisition system

The mini-climatic chamber of the Universidad de Los Andes consists of two connected containers, each one placed on one arm of the centrifuge. The first container is designed to contain water with salt to control the relative humidity and the second one is designed to contain the soil and receive the airflow. Additionally, this chamber has three infrared lamps to simulate sun radiation, a manometer and a wind sensor to simulate wind velocity, a thermocouple to measure the air temperature near the soil, and a relative humidity sensor. A module ADAM 4561 is connected to register the measurements of all sensors. The subsystems of the climatic chamber are depicted in Figure 2 and explained next.

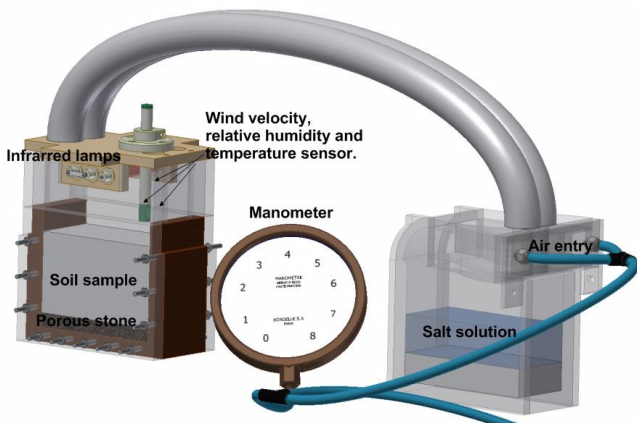


Figure 2. Mini climatic chamber.

2.2.1 Sun radiation sub-system

The sun radiation sub-system consists of a series of three infrared lamps of 200W, each one with a length of 10 centimeters. The lamps are located at the top of the soil container. The emitted radiation by the lamps was calculated using a steel plate, with a known specific heat, placed under the lamps.

Applying different electrical power to the lamps, the temperature of the plate was measured during 1200s using an infrared camera. The radiation emitted by the lamps is calculated based on the equations 1-3.

$$\frac{dT}{dt} = \frac{q_{rad} - q_{th}}{cm} \quad (1)$$

where q_{rad} = radiation flux, q_{th} = thermal emission of the plate, c = specific heat of plate, and m is the mass plate. Replacing q_{rad} and q_{th} equation 1 becomes:

$$\frac{dT}{dt} = \frac{\alpha_s I - A_s \varepsilon \sigma T_s^4}{cm} \quad (2)$$

where α_s = surface radiation absorptivity of the plate taken as 0.9 (Cohen & Doner, 1971), dT = change in temperature, dt = change in time, A_s = area of the plate, ε = emissivity coefficient at the surface, T_s = surface temperature, and σ = Stefan-Boltzmann constant. Finally, equation 3 provides the irradiance emitted by the lamps as:

$$I = \frac{1}{\alpha_s} \left(cm \frac{dT}{dt} + A_s \varepsilon \sigma T_s^4 \right) \quad (3)$$

The heat emitted by the lamps is controlled by the power supplied and the calibration values are shown in table 2.

Table 2. Electrical power supply and Infrared radiation by the lamps.

Electrical power	IR by the lamps
%	W/m ²
25	137.6
37.5	265.6
50	802.5
62.5	1354.9
75	1858.9

2.2.2 Wind velocity sub-system

Wind velocity is controlled by a manometer that regulates the air pressure. For the tests, the air source provided by the laboratory of Geotechnical models was used. A wind velocity sensor is placed at 1cm from the soil surface (Fig. 2). The calibration curve for wind velocity is shown in Figure 3.

2.2.3 Relative humidity sub-system

The relative humidity is controlled by the container with a solution of salts. Depending on the relative humidity required by the simulation, water and specific salts must be mixed in different proportions. In order to simulate real conditions, the relative humidity was selected between 72% and 86%, which corresponds to the conditions of Bogotá (IDEAM, 2008) the salt used in this research was sodium chloride NaCl.

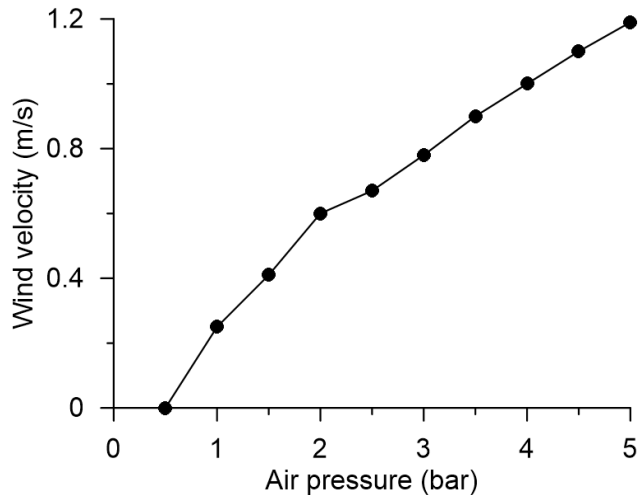


Figure 3. Calibration curve for wind velocity.

According to the proportions of salts specified by Omega, 2005, 400ml of water was mixed with 450 g of sodium chloride. Three tests were conducted with this solution. One box of the chamber was conditioned with the salt solution and the other box was filled with three different materials. The first used water reaching a relative humidity of 83%, the second used expanded polystyrene reaching 65% relative humidity, and the third used kaolin reaching 90% relative humidity.

3 PRELIMINARY RESULTS OF DESICCATION TEST

In this section, the preliminary results in soil with the mini-climatic chamber are described. All of them conducted at one gravity. Table 3 shows the selected values for the tests, which correspond to the maximum and minimum values of calibration specified in Section 2. For all tests, sodium chloride was used to simulate relative humidity as previously described. The measurements of the evaporated water were performed using an electronic scale each two hours.

Table 3. Test specifications.

Test	Radiation	Wind Velocity
	W/m^2	m/s
T1	1550.9	0.98
T2	109.6	0.3
T3	109.6	0.98
T4	1550.9	0.3

3.1 Effect of wind velocity on desiccation

Figure 4-5 show the water evaporation curves for the models with the same emitted infrared radiation. Figure 4 depicts the results for an infrared radiation of $1550.9 W/m^2$ and Figure 5 for $109.6 W/m^2$.

For potential evaporation, it was expected that the tests T1 and T3, with highest wind velocity, show higher evaporation rate than the tests T2 and T4, with lowest wind velocity (Penman, 1948).

This trend is in accordance with the obtained results, but the difference in the evaporation rate between the two wind velocities is higher for the lowest values of radiation. For higher values of radiation the effect of wind velocity seems not be as significant.

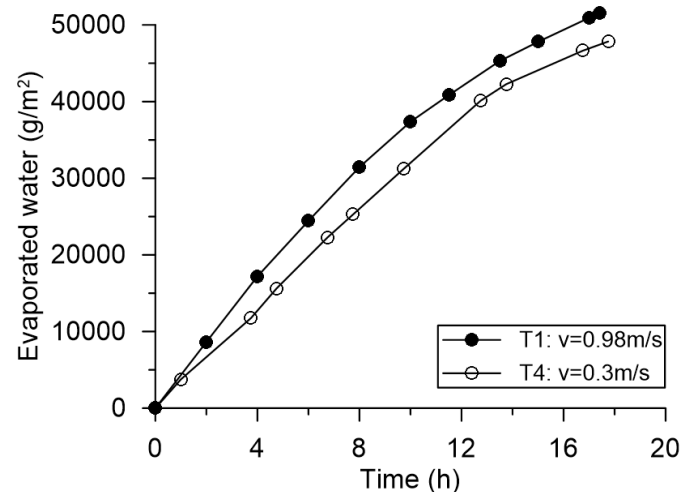


Figure 4. Evaporated water comparison between two test using the highest radiation $1550.9 W/m^2$ and different wind velocity.

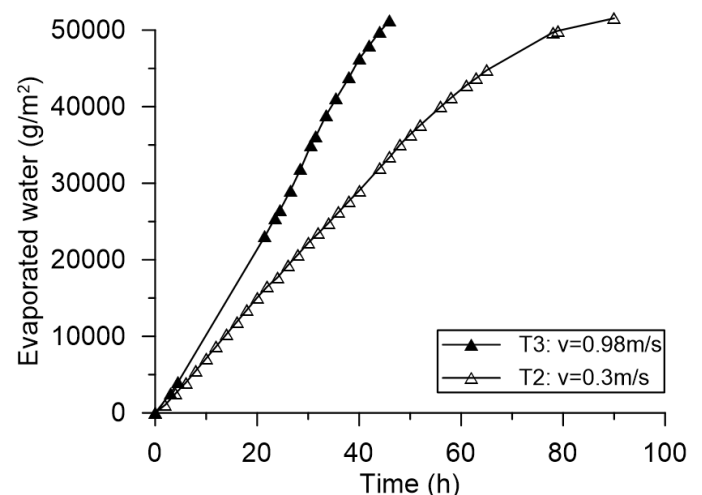


Figure 5. Evaporated water comparison between two test using the lowest radiation 109.6 W/m² and different wind velocity.

3.2 Effect of radiation on desiccation

Figure 6-7 show the same tests described before. In this case, evaporation curves are plotted using the same wind velocity and different emitted radiation. The evaporation rates for these curves evidence the main effect of radiation on evaporation.

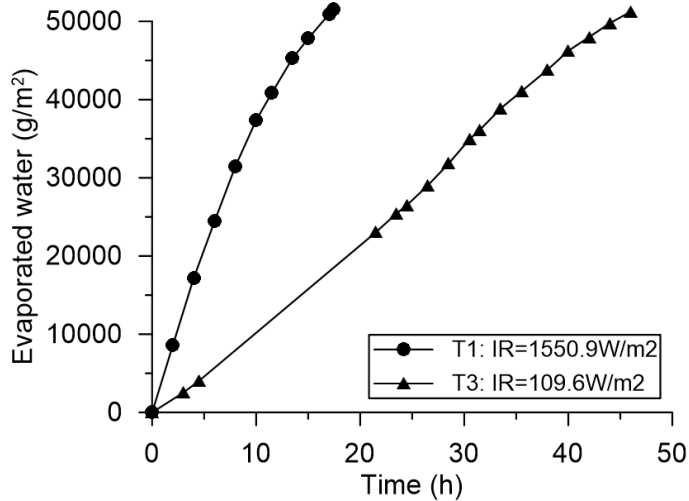


Figure 6. Evaporated water comparison between two test using wind velocity of 0.98 m/s and different radiation.

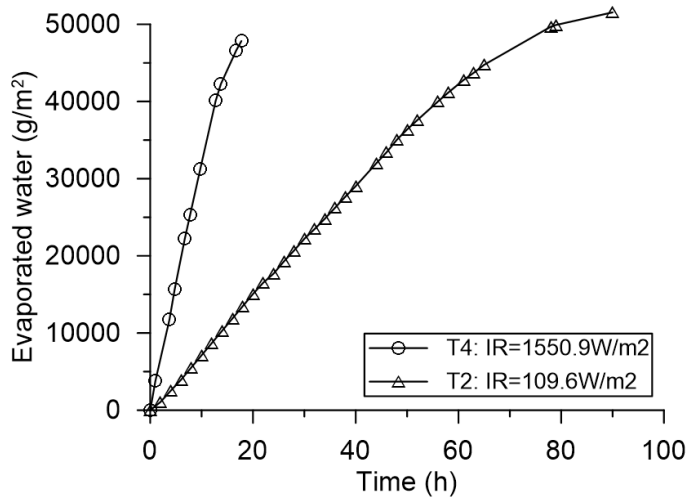


Figure 7. Evaporated water comparison between two test using wind velocity of 0.3 m/s and different radiation.

4 DESICCATION CRACKS

As it is shown in Figure 8-11 cracks were developed as desiccation occurred. These desiccation cracks started at the surface propagating to the bottom of the container.



Figure 8. Crack formation. Test T1.



Figure 9. Crack formation. Test T2.



Figure 10. Crack formation. Test T3.

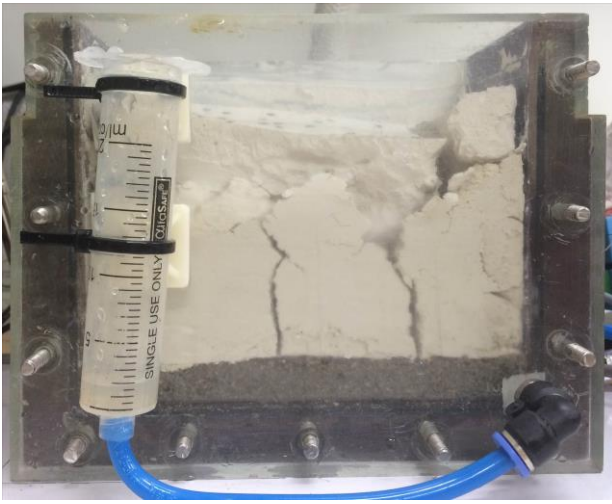


Figure 11. Crack formation. Test T4.

5 CONCLUSIONS

A new climatic chamber for modelling soil drying was developed at the Universidad de los Andes in Bogotá, Colombia. Preliminary desiccation tests were conducted at one gravity to determine the influence of wind velocity and sun radiation on evaporation.

As a result, the influence of wind velocity is higher in the experiments made with lower radiation leading to a state that the evaporation rate depends more on the radiation impinged in the soil than of the effect of wind velocity. Additionally, desiccation cracks were registered in all models started from the surface.

Many tests have to be conducted in order to completely characterize the effect of wind velocity, infrared radiation, and relative humidity on desiccation and cracking process. Additionally, further research is needed in the scaling of environmental variables in centrifuge and the effect of a real stress state.

Next investigations will be made in the new environmental chamber adapted to the geo-centrifuge. A comparison of the $1\times G$ and $N\times G$ results will be made in order to establish the effect of the stress in the soil and the scaling laws of the environmental variables.

6 REFERENCES

Abu-Hejleh, A. N., & Znidarcic, D. 1995. Desiccation theory for soft cohesive soils. *Journal of Geotechnical Engineering*, 121(6), 493-502.

Caicedo, B., J. Tristanco, & Luc Thorel. "Centrifuge modeling of soil atmosphere interaction using a climatic chamber." *Physical Modelling in Geotechnics* (2010): 299-305.

Cohen, M., & Doner, J. P. 1971. *Infrared reflectance spectra for selected paint pigments*. Springfield: National technical information service.

Corte, A., & Higashi, A. 1960. *Experimental research on desiccation cracks in soil*. U.S. Army now, Ice and Permafrost Research Establishment, Hanover, N.H. Research report 66.

IDEAM. 2008. *Estudio de la Caracterización Climática de Bogotá y Cuenca Alta del Rio Tunjuelo*. Bogotá: Alcaldía mayor de Bogotá.

IPCC. 2014. *Summary for policymakers*. En: *Climate Change 2014: Impacts, Adaptation, and Vulnerability. Part A: Global and Sectoral Aspects. Contribution of Working Group II to the Fifth Assessment Report of the Intergovernmental Panel on Climate Change* [Field, C.B., V.R. Barros, D.J. Dokken, K.J. Mach, M.D. Mastrandrea, T.E. Bilir, M. Chatterjee, K.L. Ebi, Y.O. Estrada, R.C. Genova, B. Girma, E.S. Kissel, A.N. Levy, S. MacCracken, P.R. Mastrandrea, and L.L. White (eds.)]. Cambridge University Press, Cambridge, Reino Unido y Nueva York, NY, EE.UU, pp. 1-32.

Lozada, C., Caicedo, B., & Thorel, L. 2015. Effects of cracks and desiccation on the bearing capacity of soil deposits. *Geotechnique letters*, 5, 112-117.

Miller, C.J., Mi, H., & Yesiller, N. 1998. Experimental analysis of desiccation crack propagation in clay liners. *Journal of the American Water Resources Association*, 34, No. 3, 677-686.

Nahlawi, H., & Kodikara, J. K. 2006. Laboratory experiments on desiccation cracking of thin soil layers. *Geotechnical & Geological Engineering*, 24(6), 1641-1664.

Omega. Equilibrium relative humidity. Download from: <http://www.omega.com/temperature/z/pdf/z103.pdf>. October 15 2015

Penman, H.L., 1948, April. Natural evaporation from open water, bare soil and grass. In *Proceedings of the Royal Society of London A: Mathematical, Physical and Engineering Sciences* (Vol. 193, No. 1032, pp. 120-145). The Royal Society.

Take, W. A., & Bolton, M. D. 2002. An atmospheric chamber for the investigation of the effect of seasonal moisture changes on clay slopes. In *Proc., Int. Conf. on Physical Modeling in Geotechnics* (pp. 765-770). Rotterdam, The Netherlands: Balkema.

Thusyanthan, N. I., Take, W. A., Madabhushi, S. P. G., & Bolton, M. D. 2007. Crack initiation in clay observed in beam bending. *Geotechnique*, 57(7), 581-594.

Song, W. K., Cui, Y. J., Tang, A. M., Ding, W. Q., & Tran, T. D. 2013. Experimental study on water evaporation from sand using environmental chamber. *Canadian Geotechnical Journal*, 51(2), 115-128.

Trabelsi, H., Jamei, M., Zenzri, H., & Olivella, S. 2012. Crack patterns in clayey soils: Experiments and modeling. *International Journal for Numerical and Analytical Methods in Geomechanics*, 36(11), 1410-1433.

Vesga, L., Caicedo, B., & Mesa, L. 2003. Deep Cracking in Sabana de Bogotá Clay. *Proceedings of the Twelfth Panamerican Conf. on Soil Mech. and Geotech. Engineering*. Cambridge, Mass, pp. 737-742.